



Practical and controlled laboratory vibration experiments that demonstrate the impulsive response of multi-staged clutch dampers

Michael D. Krak^a

Rajendra Singh^b

Acoustics and Dynamics Laboratory, NSF Smart Vehicle Concepts Center, Department of Mechanical and Aerospace Engineering, The Ohio State University, Columbus, Ohio, USA

Many vehicle powertrain sub-systems contain highly non-linear torsional devices such as multi-staged clutch dampers. These devices transmit torque and isolate torsional vibration from the engine to the transmission, and are intentionally designed to possess several non-linear features such as multi-staged stiffness and friction elements, pre-loads, clearances, and asymmetry. It is evident that linear models are not sufficient to fully describe these devices, especially when considering the impulsive response. The understanding of these devices and the development of non-linear vibration simulation tools can be facilitated by experimental measurements. This paper proposes two laboratory experiments; both are non-rotating and non-linear systems excited by a step-like external torque. The first is a large scale experiment which accommodates production clutch dampers. The second is a controlled benchtop experiment which includes a single clearance and a scaled linearized clutch damper in the form of a torsional spring. The transient vibration response of each system is measured using a laser vibrometer and translational accelerometers. Distinct characteristics of vibration responses, such as impact regime and period behavior, are identified and related to corresponding design features. This experimental study will aid in acquiring an improved understanding of several transient noise and vibration sources in vehicles and rotating machines.

1 INTRODUCTION

Torsional devices typically have clearances by design (say a backlash or multi-staged element) or otherwise (assembly error, machining tolerances, or wear). An example of such a device is the multi-staged clutch damper in ground vehicles¹⁻⁶, though many applications can be found in aerospace, power plant, mining, and appliance industries. The clutch damper serves to mainly transmit torque in vehicle powertrains, while isolating torsional oscillations between the flywheel and transmission input shaft. This device must operate over a wide range of torque

^a email: krak.6@osu.edu

^b email: singh.3@osu.edu

loads (idling to driving conditions) and thus is intentionally designed to contain several discontinuous non-linear characteristics, such as multi-staged stiffness, multi-staged friction elements, pre-load features, clearances, and asymmetry¹⁻⁶. These features are illustrated by quasi-static performance curves, such as the example shown in Fig. 1, where θ is the relative angular displacement between a flywheel and transmission input shaft, T_D is the transmitted torque, K_D is the torsional stiffness, and H_D is the frictional hysteresis.

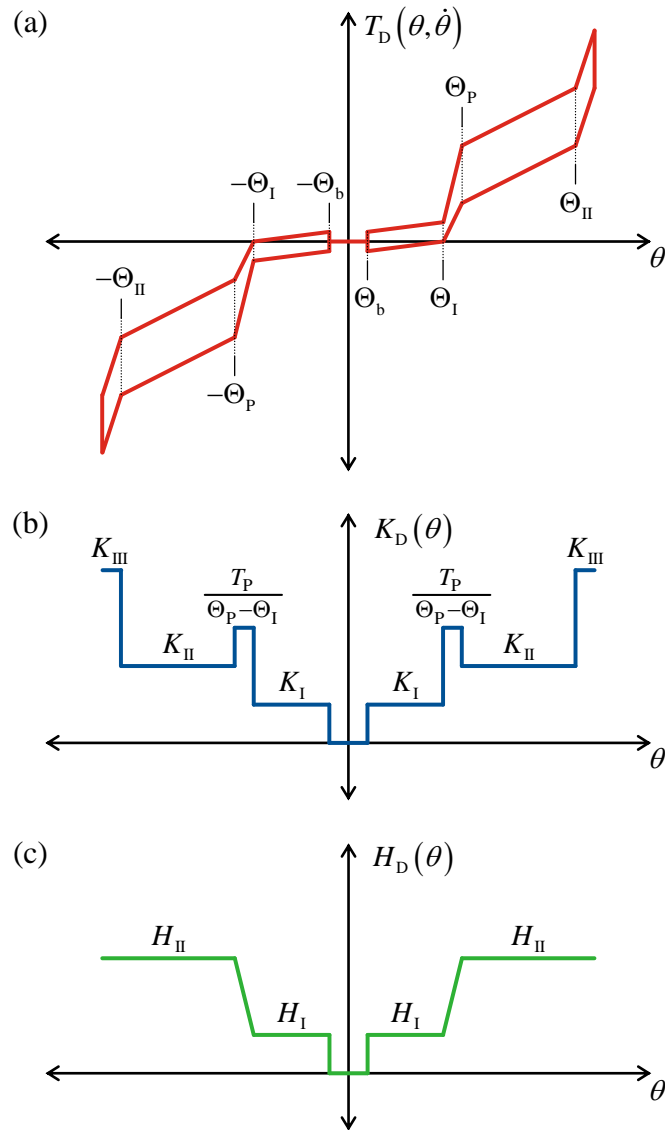


Fig. 1 – Quasi-static performance curves of a multi-staged clutch damper: (a) transmitted torque T_D , (b) torsional stiffness K_D , and (c) frictional hysteresis H_D where θ is relative angular displacement between a flywheel and transmission input shaft. Key: K – torsional stiffness, H – frictional hysteresis, Θ – clearance or stage transition (angular), (I, II, III) – stage index, b – clearance, and T_P – pre-load.

Due to the presence of clearance and/or stage transitions, these devices are susceptible to vibro-impacts, which are a major source of noise and vibration. Three vibro-impact types are

possible. First, consider the no-impact case, which occurs when the dynamic motion about a given mean operating point is not sufficient to cross a transition. The second type, termed rattle, occurs when the pulsating motion about the mean operating point crosses one (single-sided impact) or two (double-sided impact) transitions⁴. The third type is clunk, which is associated with the mean operating point abruptly changing and the resulting in dynamic motion crossing one or two transitions⁵⁻⁷. See Krak et al.^{8,9} for further details.

Improvement of torsional devices could be facilitated by a better understanding of the physics that includes the estimation and selection of parameters (for both static and dynamic conditions), identification of dissipative mechanisms, and definition of pre-load features. To accomplish these goals, benchmark measurements are needed, though there is a lack of controlled experiments. Prior efforts include the work of Couderc et al.² who proposed a rotating experiment that captures the behavior of a production multi-staged clutch damper coupled to a transmission during engine run-up. Further, Gurm et al.⁶ and Crowther et al.⁷ proposed vibratory experiments that demonstrate the impulsive (clunk-like) response of a production driveline (without a clutch damper). However, prior work^{2,6,7} incorporates production devices with somewhat controllable or unknown non-linear elements. In order to better investigate a single non-linear feature, say a clearance, a controlled laboratory experiment is needed, such as ones proposed by Todd et al.¹⁰, Wierchigroch et al.¹¹, and Ing et al.¹².

Therefore, the purpose of this article is to achieve the following two objectives: 1. Propose a vibratory experiment that demonstrates the impulsive response of a production multi-staged clutch damper (denoted E1); and 2. Propose a controlled scaled vibratory experiment that demonstrates the impulsive response of a torsional system with a single clearance element (denoted E2). An attempt will be made to identify distinct characteristics of the measured impulsive responses and relate them to design features (in both experiments).

2 CONCEPTUAL DESCRIPTION OF THE TWO EXPERIMENTS

The proposed vibratory experiments are conceptually illustrated in Fig. 2. Both E1 and E2 are torsional non-linear systems that are excited by an external step-like torque, similar to prior work^{6,7}. However, the most significant difference between the two systems is the number of designed non-linear features, as summarized in Table 1. Experiment E1 incorporates a practical device which, as previously stated, has many known and unknown non-linear features that are not easily controlled. However, E2 is a scaled-down version of E1 and is intentionally designed to contain only one known and controllable non-linear feature (clearance).

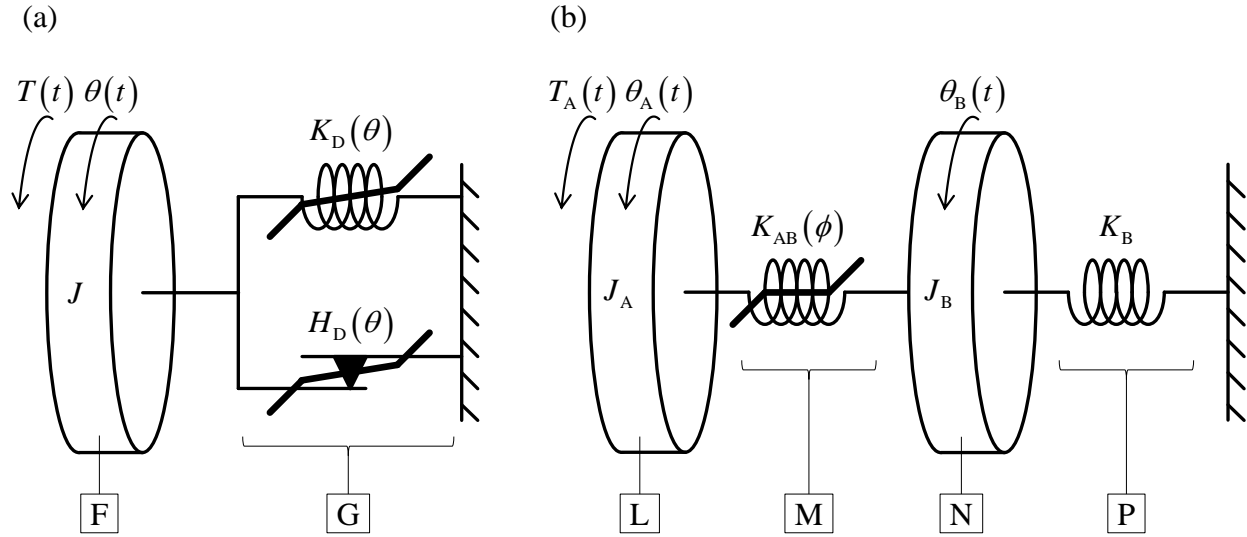


Fig. 2 – Conceptual models of two proposed experiments: (a) E1 and (b) E2. Key: F – torsion arm, shaft, and spline (E1), G – multi-staged clutch damper, L – torsion arm and shaft (E2), M – key and keyway, N – jaw-coupling hub, and P – torsional spring.

Table 1 – Summary of non-linear design features of experiments E1 and E2.

Non-linear feature	Experiment E1	Experiment E2
Clearance element	✓	✓
Multi-staged stiffness	✓	
Pre-load	✓	
Multi-staged friction	✓	

Experiment E1 can be described as a single degree of freedom (1DOF) torsional system for design purposes. The system consists of a torsional inertia J (rigid torsion arm, shaft, and spline) which has angular motion $\theta(t)$. Inertia J is coupled to ground through a multi-staged stiffness K_D and multi-staged friction element H_D (production multi-staged clutch damper). The following assumptions are made regarding the clutch damper: the device can be described by Fig. 1; stage I is effectively a clearance ($K_I \approx 0$); all stiffness and hysteresis parameters can be estimated from measured quasi-static torque curves; and the torsional inertia of the device (J_D) is negligible ($J \gg J_D$). Also, damping is assumed to be negligible for simplicity.

Experiment E2 can be described as a two degree of freedom (2DOF) torsional system for design purposes. The system consists of torsional inertias J_A (rigid torsion arm and shaft) and J_B (jaw coupling hub), which have angular motions $\theta_A(t)$ and $\theta_B(t)$ respectively. Inertias J_A and J_B are coupled together through a clearance element $K_{AB}(\phi)$ (keyway), where $\phi(t) = \theta_A(t) - \theta_B(t)$, and J_B is coupled to ground through stiffness K_B (torsional spring). It is assumed that the stiffness of $K_{AB}(\phi)$ is very high ($K_{AB} \gg K_B$) and is considered rigid for design purposes. Again, damping is assumed to be negligible for simplicity.

3 EXPERIMENT E1

A physical illustration of experiment E1 is provided in Fig. 3. For simplicity, a flywheel is chosen as ground. A clutch assembly, which houses a sleeve bearing and a multi-staged clutch damper, is bolted to the flywheel. The clutch damper couples to a shaft through a spline connection. The shaft is radially supported by the sleeve bearing and a ball bearing exterior to the clutch assembly. A torsion arm is rigidly attached to the shaft; a pneumatic actuator with a mechanical quick release is located at the free end of the torsion arm.

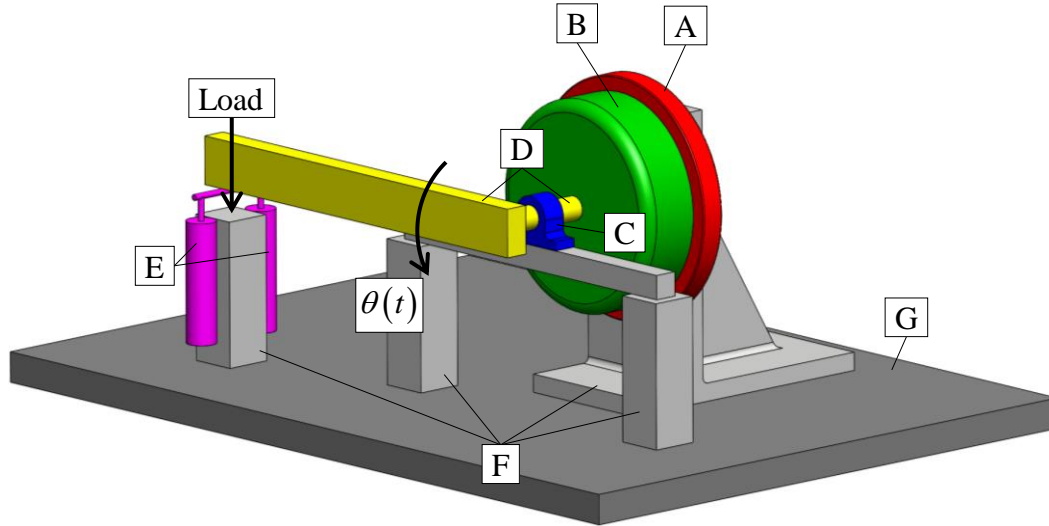


Fig. 3 – Physical illustration of experiment E1. Key: A – flywheel, B – clutch assembly (houses a sleeve bearing and multi-staged clutch damper), C – ball bearing, D – torsion arm and shaft (J), E – pneumatic actuation system with a mechanical quick release, F – structural supports (ground), and G – bedplate (ground).

Inertia J is determined by the natural frequency of an equivalent, 1DOF linear system with inertia J and stiffness K_{II} . The desired natural frequency is about 10 Hz because the impulsive response of a vehicle driveline is closely related to the torsional surge mode, which occurs between 5 to 15 Hz^{6,7}. Therefore, J is chosen to satisfy $J \approx K_{II} / (20\pi)^2$. The external torque $T(t)$ is provided by the pneumatic actuator and mechanical quick release. The time history of $T(t)$ has a step-like transition from initial value T_0 (for $t \leq 0$) to final value T_f (for $t > 0$). To ensure a non-linear response, the initial operating point (θ_0, T_0) is chosen to lie on stage II, and the final operating point (θ_f, T_f) is chosen to lie on stage I or the pre-load.

A schematic of the instrumentation system for E1 is given in Fig. 4. The angular displacement of the arm is defined by $\theta(t)$ (w.r.t. the clutch damper datum) and $\psi(t)$ (w.r.t. to horizon). Dynamic angular motion is not measured, but is instead calculated from measured translational motion. A laser vibrometer is chosen to measure the translational velocity $\dot{v}(t)$, which is parallel to the horizon. The instantaneous radial distance from the shaft to the laser point is denoted by $L_v(t)$. The translational acceleration ($\ddot{w}(t)$) of a point on J is measured by an accelerometer; it is assumed that $\ddot{w}(t)$ is tangential to the angular motion of J . Dynamic strain in the torsion arm $\varepsilon'(t)$ is measured by a strain gage located on the top-side of the arm. Signals $\dot{v}(t)$ and $\ddot{w}(t)$ are sampled separately (though simultaneously) from $\varepsilon'(t)$ due to hardware constraints; all signals are sampled at a frequency of 1.28 kHz.

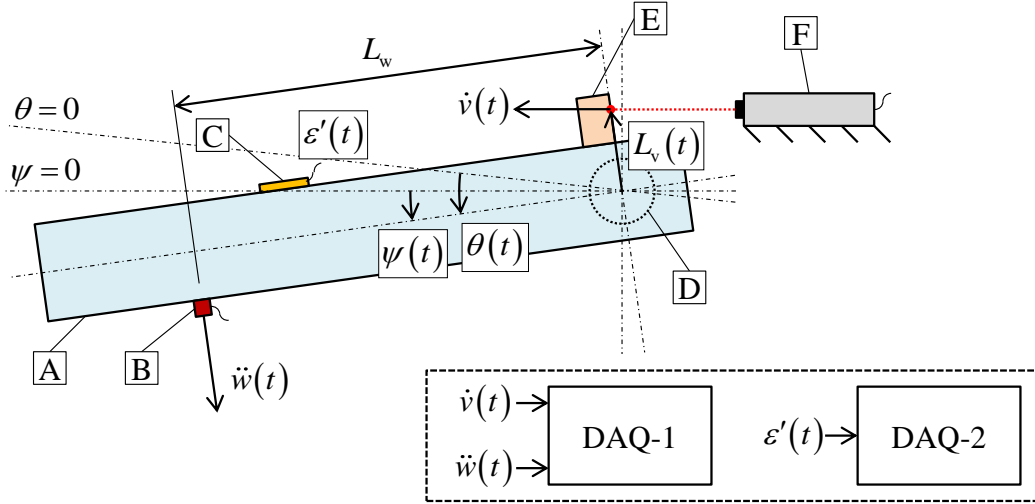


Fig. 4 – Instrumentation schematic for experiment E1. Key: A – torsion arm, B – translational accelerometer, C – strain gage, D – shaft, E – measurement surface for the laser, F – laser vibrometer, and DAQ – data acquisition system.

Prior to excitation ($t < 0$), the torsion arm is loaded with torque T_0 and initial conditions are measured, such as ψ_0 , L_{v0} , and v_0 (initial translational displacement of the laser point). The excitation is then applied (at $t = 0$) and signals $\dot{v}(t)$, $\ddot{w}(t)$, and $\varepsilon'(t)$ are measured; position ψ_f is measured after the system reaches equilibrium. Translational displacement $v(t)$ is calculated by numerically integrating $\dot{v}(t)$; angular displacement $\theta(t)$ is then calculated by the following where θ_f is determined by the static balance of T_f

$$L_v(t) = \left[L_{v0}^2 + (v_0 - v(t))^2 + 2L_{v0}(v_0 - v(t))\sin(\psi_0) \right]^{0.5}, \quad (1)$$

$$\theta(t) = \theta_f + \psi_0 - \psi_f - \sin^{-1} \left[(v_0 - v(t))\cos(\psi_0)/L_v(t) \right]. \quad (2)$$

Angular acceleration $\ddot{\theta}(t)$ is calculated using the following

$$\ddot{\theta}(t) = \ddot{w}(t)/L_w. \quad (3)$$

Synchronized dynamic strain is defined by $\varepsilon(t) = \varepsilon'(t - t_{\text{lag}})$ where t_{lag} is determined from the cross-correlation of $\varepsilon'(t)$ and $-\ddot{\theta}(t)$. Further details on design and instrumentation are given by Krak et al.^{8,9}

The measured responses for experiment E1 are given in Fig. 5. Angular motion and time are normalized by transition Θ_b and natural frequency f_n ; dynamic strain is normalized by its maximum value. The response has three distinct response regimes: double-sided impact (DS), single-sided impact (SS), and no-impact (NI). These regimes can be defined by motion with respect to $\bar{\Theta}_1$ and $-\bar{\Theta}_1$, which are the transitions from very low stiffness ($K_1 \approx 0$) to high stiffness as shown by $\bar{\varepsilon}(\bar{\theta})$. The double-sided impact regime occurs when travel crosses both $\bar{\Theta}_1$ and

$-\bar{\Theta}_1$, which corresponds to significant positive and negative values of $\bar{\theta}(\bar{t})$. The single-sided impact regime occurs when travel crosses $\bar{\Theta}_1$ only, which corresponds to significant negative values of $\bar{\theta}(\bar{t})$. The no-impact regime occurs when the travel does not cross either $\bar{\Theta}_1$ or $-\bar{\Theta}_1$; though the response is non-linear, it appears sinusoidal.

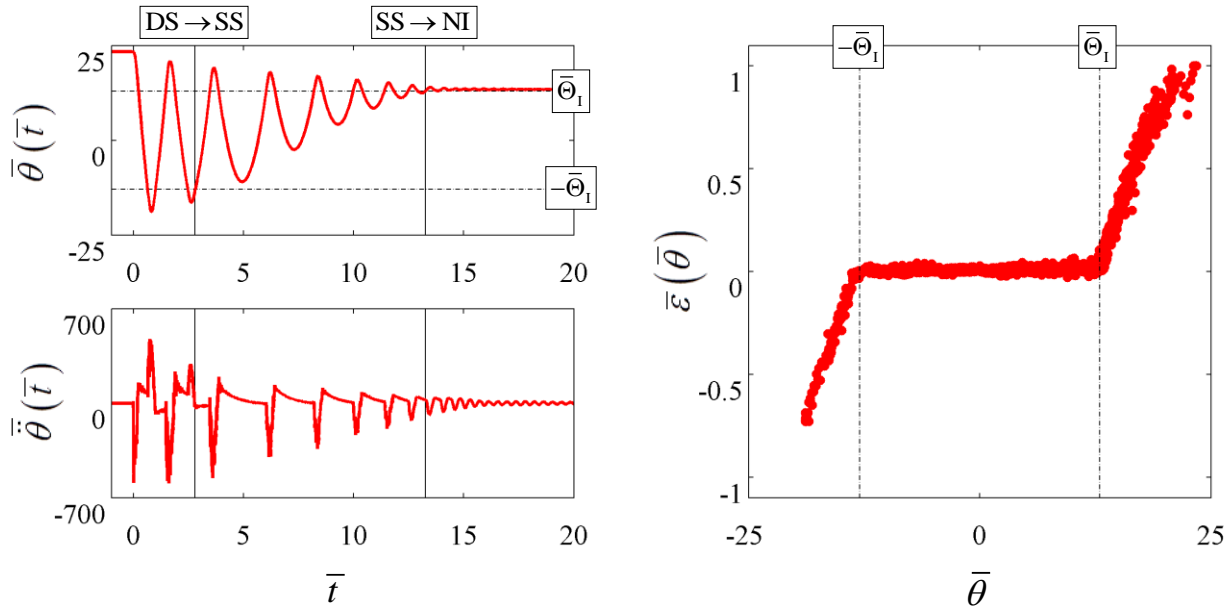


Fig. 5 – Measured responses of experiment E1. Key: (—) – measurement, (|) – response regime transition, (---) – stage or clearance transition, DS→SS – transition from double-sided to single-sided impact regime, SS→NI – transition from single-sided impact to no-impact regime, and $\pm\bar{\Theta}_1$ – stage I transition.

4 EXPERIMENT E2

A physical illustration of experiment E2 is given in Fig. 6. A set of jaw-coupling hubs is selected; one hub is grounded and the other (J_B) is free to vibrate. The elastomer spider between the jaws is removed and replaced with coil springs (K_B). A shaft and torsion arm (J_A) connect to the coupling hub (J_B) through a key and keyway ($K_{AB}(\phi)$). The shaft is radially supported by a sleeve bearing. A small steel disk is rigidly attached to the end of the torsion arm; this disk is the attachment point for an electromagnet and mass.

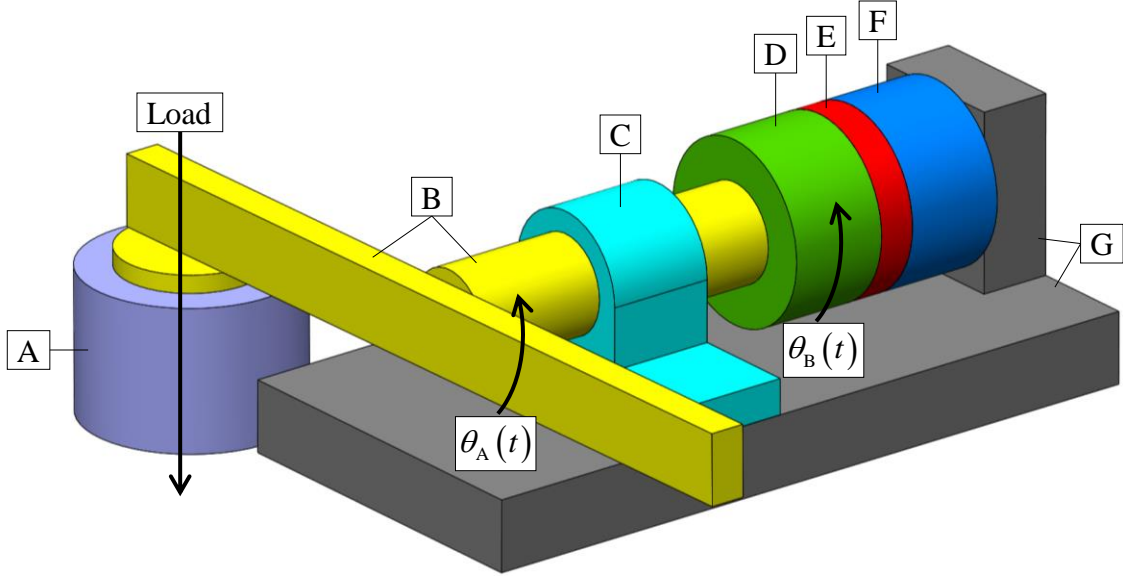


Fig. 6 – Physical illustration of experiment E2. Key: A – electromagnet and mass, B – torsion arm and shaft (J_A), C – sleeve bearing, D – jaw-coupling hub (J_B), E – torsional spring, F – jaw-coupling hub (ground), and G – bedplate (ground).

Like E1, the components of experiment E2 are sized using the natural frequency (f_n) of an equivalent linear system, which has inertia $J_A + J_B$ and stiffness K_B . Again, the desired natural frequency is roughly 10 Hz. Inertia J_B and stiffness K_B are manufactured components with known values; therefore, J_A must satisfy $J_A \approx K_B / (20\pi)^2 - J_B$. The external torque $T_A(t)$ is supplied by an electromagnet-mass drop, which occurs at $t = 0$. The initial torque value T_{A0} is controlled by the overhanging mass of the electromagnet; the final torque value T_{Af} is negligible due to the symmetry of the torsion arm. The final operating point (ϕ_f, T_{Af}) is very near the clearance transition point ($\Phi_b, 0$), and the initial operating point (ϕ_0, T_{A0}) is relatively distant.

Accelerometers are chosen to measure translational accelerations on J_A and J_B ($\ddot{u}_A(t)$ and $\ddot{u}_B(t)$, respectively). The radial distances from the axis of rotation to the accelerometers are denoted L_{uA} and L_{uB} . It is assumed that both $\ddot{u}_A(t)$ and $\ddot{u}_B(t)$ are tangential to the angular motions of J_A and J_B . Prior to excitation ($t < 0$), the system is loaded with torque T_{A0} (electromagnet and mass). The excitation is applied (at $t = 0$) by stopping the electrical current to the electromagnet through a switch. Then, signals $\ddot{u}_A(t)$ and $\ddot{u}_B(t)$ are sampled at a frequency of 1.28 kHz. The angular accelerations $\ddot{\theta}_A(t)$ and $\ddot{\theta}_B(t)$ are calculated using the following

$$\ddot{\theta}_A(t) = \ddot{u}_A(t) / L_{uA}, \quad \ddot{\theta}_B(t) = \ddot{u}_B(t) / L_{uB}. \quad (5a-b)$$

The measured responses of experiment E2 are given in Fig. 7; acceleration and time are normalized by the clearance transition Φ_b and natural frequency f_n . The response is in the double-sided impact regime (DS), which is characterized by travel across clearance transitions Φ_b and $-\Phi_b$. It is not necessary to calculate or measure angular displacement because E2 is designed to contain only one clearance. When contact is made at the clearance, there are

corresponding negative and positive peak values in the angular acceleration signals $\bar{\bar{\theta}}_A(\bar{t})$, $\bar{\bar{\theta}}_B(\bar{t})$, and $\bar{\bar{\phi}}(\bar{t})$.

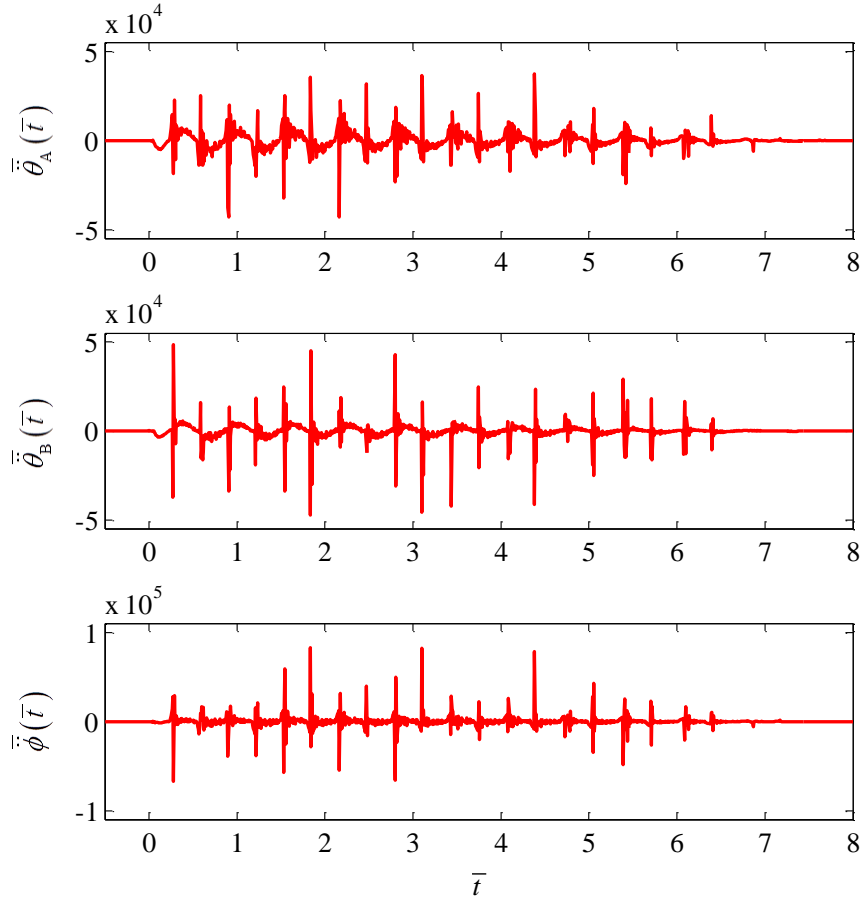


Fig. 7 – Measured responses of experiment E2, where $\bar{\bar{\phi}}(\bar{t}) = \bar{\bar{\theta}}_A(\bar{t}) - \bar{\bar{\theta}}_B(\bar{t})$.

5 CONCLUSION

This paper proposes two vibratory experiments that demonstrate the impulsive response of a torsional system with a clearance or multi-staged stiffness element. The first experiment (E1) incorporates a production multi-staged clutch damper which has several non-linear features, including multi-staged stiffness, multi-staged friction elements, pre-load features, and clearances. The second experiment (E2) is a scaled-down version of E1 and it is designed to contain only one known controllable non-linear (clearance) element. The measured responses of both experiments exhibit distinct and rich non-linear response regimes, such as double-sided impact, single-sided impact, and no-impact regimes. The measurements also show that the transition between response regimes and the location of peak angular acceleration corresponds to the well-defined clearance or stage transitions. Measurements provide much physical insight and useful benchmark data that could be utilized to validate mathematical models.

6 ACKNOWLEDGEMENTS

The authors acknowledge Eaton Corporation (Clutch Division) for supporting this research. We would like to thank Luiz Pereira and Brian Franke for their assistance with experimental studies. Further, we acknowledge the member organizations of the Smart Vehicle Concepts Center (www.SmartVehicleCenter.org) and the National Science Foundation Industry/University Cooperative Research Centers program (www.nsf.gov/eng/iip/iucrc) for partially supporting this basic research.

7 REFERENCES

1. F. Shaver, Manual Transmission Clutch Systems, (SAE, 1997).
2. P. Couderc, J. Callanaere, J. Der Hagopian, G. Ferraris, A. Kassai, Y. Borjesson, L. Verdillon, S. Gairnard, Vehicle driveline dynamic behavior: Experimentation and simulation, *Journal of Sound and Vibration* 218 (1) (1998) 133-157.
3. C.L. Gaillard, R. Singh, Dynamic analysis of automotive clutch dampers, *Applied Acoustics* 60 (2000) 399-424.
4. J.Y. Yoon, R. Singh, Effect of multi-stage clutch damper characteristics on transmission gear rattle under two engine conditions, *ProcIMEchE Part D: Journal of Automobile Engineering*, 277 (2013) 1273-1295.
5. W. Oh, R. Singh, Examination of clunk phenomena using a non-linear torsional model of a front-wheel drive vehicle with manual transmission, *2005 SAE Noise and Vibration Conference*, Traverse City MI, May 16-19 2005, SAE Paper 2005-01-2291.
6. J. S. Gurm, W. J. Chen, A. Keyvanmanesh, T. Abe, A. R. Crowther, R. Singh, Transient clunk response of a driveline system: Laboratory experiment and analytical studies, *SAE Transactions Journal of Passenger Cars: Mechanical Systems*, 116 (6) (2008) Paper # 2007-01-2233.
7. A.R. Crowther, R. Singh, N. Zhang, C. Chapman, Impulsive response of an automatic transmission system with multiple clearances: Formulation, simulation and experiment, *Journal of Sound and Vibration*, 306 (2007) 444-466.
8. M. D. Krak, J. T. Dreyer, and R. Singh, Development of a Non-Linear Clutch Damper Experiment Exhibiting Transient Dynamics, *SAE 2015 Noise & Vibration Conference & Exhibition*, 22-25 June 2015, Grand Rapids, MI, SAE Paper # 2015-01-2189.
9. M. D. Krak, J. T. Dreyer, R. Singh, Development and validation of an experiment which exhibits the impulsive response of a highly non-linear torsional system, *in review for Mechanical Systems and Signal Processing* (2015).
10. Todd, MD; Virgin, LN, Natural frequency considerations of an impact oscillator, *Journal of Sound and Vibration*, 194 (1996) 452-460.
11. M. Wiercigroch, V.W.T. Sin, Experimental study of a symmetrical piecewise base-excited oscillator, *Journal of Applied Mechanics*, 65 (1998) 657-663.
12. J. Ing, E. Pavlovskasia, M. Wiercigroch, Dynamics of a nearly symmetrical piecewise linear oscillator close to grazing incidence: Modelling and experimental verification, *Nonlinear Dynamics*, 46 (2006) 225-138.